JOURNAL OF SOLID STATE CHEMISTRY 88, 278–290 (1990)

Investigations on the Structural, Electrical, and Magnetic Properties of $Nd_{2-x}Sr_xNiO_{4+\delta}$

BRIAN W. ARBUCKLE, K. V. RAMANUJACHARY, ZHEN ZHANG, AND MARTHA GREENBLATT[1]

Department of Chemistry, Rutgers–The State University of New Jersey, Piscataway, New Jersey 08855-0939

Received April 5, 1990

DEDICATED TO MY GOOD FRIEND GEORGE HONIG WHOM I (MARTHA GREENBLATT) ADMIRE AS A RENAISSANCE MAN

Solid–solutions of the type $Nd_{2-x}Sr_xNiO_{4+\delta}$ ($0 \le x \le 1$) were prepared by codecomposition of the metal nitrates and were characterized by means of powder X-ray diffraction, TGA, electrical resistivity, and magnetic susceptibility measurements. $Nd_2NiO_{4+\delta}$ possesses orthorhombic symmetry at ambient temperatures and exhibits a phase transition to pseudo-tetragonal symmetry upon doping with Sr^{2+} ($x \approx 0.2$). The tetragonality ratio c/a_t measured as a function of x shows an anomalous increase at $x \approx 0.2$ and a maximum near $x = 0.6$. Considerable deviation from oxygen stoichiometries was observed in the orthorhombically distorted members, while for the samples with tetragonal geometry the oxygen contents were near the ideal value. All the samples, except $NdSrNiO_4$, were semiconducting from room temperature down to 10 K. $NdSrNiO_4$ showed a metal–semiconductor transition at ~190 K. The magnetic susceptibility shows Curie–Weiss behavior with an onset of long range antiferromagnetic ordering ($T_N = 17$ K) in some of the intermediate members of the solid–solution series. The effect of Sr^{2+} substitution on the structural and electronic properties of $Nd_{2-x}Sr_xNiO_{4+\delta}$ are discussed in terms of the mixed valence character of Ni^{2+}/Ni^{3+}, distortions in the local coordination of Ni–O octahedra, and correlation effects of $d_{x^2-y^2}$ bands in the Ni–O basal plane.

Introduction

Rare earth nickel oxides with the general formula $Ln_2NiO_{4+\delta}$ (Ln = La, Pr, or Nd), are known to crystallize with K_2NiF_4-type structure, which can be described as alternating perovskite $LnNiO_3$ and rock salt LnO layers stacked along the crystallographic c-axis (Fig. 1). The Ni–O octahedral units share corners in the ab plane forming a two-dimensional network which give these compounds interesting anisotropic properties, i.e., the electrical transport and magnetic exchange interactions in $La_2NiO_{4+\delta}$ are confined within the Ni–O basal plane (*1–4*).

Rare earth nickelates show a considerable range of oxygen nonstoichiometry depending upon their synthetic preparation. The excess oxygen has been attributed to intergrowths of Ruddlesden–Popper-type phases (*5*), deviations in the metal–ion ratio (*6*), variable valence of the transition metal ion (*7*), and more recently to the incorporation of interstitial oxygen defects (*8*). The structural and electronic properties of $Ln_2NiO_{4+\delta}$-type compounds are reported to be extremely sensitive to the deviations in the oxygen stoichiometry (*2, 4, 9, 10*). For ex-

[1] To whom correspondence should be addressed.

0022-4596/90 $3.00

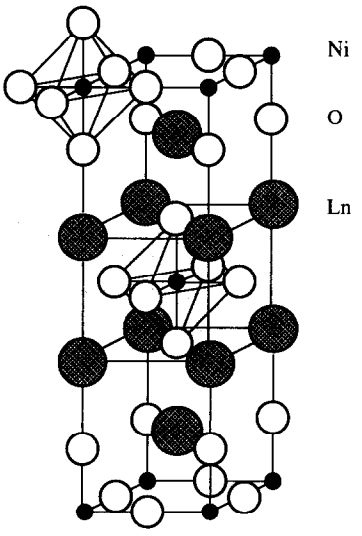

FIG. 1. Tetragonal K_2NiF_4 type structure of Ln_2NiO_4, Ln = La, Nd, or Pr.

ample, the nonstoichiometric $La_2NiO_{4+\delta}$ is tetragonal at ambient temperatures while the nearly stoichiometric La_2NiO_4 shows orthorhombic distortion. Nonstoichiometric $Nd_2NiO_{4+\delta}$ and $Pr_2NiO_{4+\delta}$ undergo an orthorhombic to tetragonal phase transition at 724 and 834 K, respectively, whereas $La_2NiO_{4+\delta}$ shows no evidence of a phase transition up to 1073 K (*11*). Electrical conductivity studies on $La_2NiO_{4+\delta}$ show a semiconductor-to-metal transition between 500 and 620 K (*3, 12*). Goodenough and Ramasesha have suggested that the large spread of transition temperature values may be due to the variations in the oxygen stoichiometry (*13*). It has also been found that by increasing δ in $Nd_2NiO_{4+\delta}$ and $Pr_2NiO_{4+\delta}$, the magnetic ordering is suppressed (*4*).

It is reported that $Nd_2NiO_{4+\delta}$ can have either monoclinic (*14*) or orthorhombic symmetry (*15*). The source of the structural difference is unclear; it may be due to the oxygen content or structural defects. It has also been reported that $NdSrNiO_4$ has tetragonal symmetry (*16, 17*). It was thought that the substitution of Sr for Nd in $Nd_2NiO_{4+\delta}$ might induce a structural phase transition from orthorhombic to tetragonal symmetry and would induce mixed valency for the transition metal ion, which would in turn induce interesting electrical and magnetic properties in this system. Therefore, a structural, electrical, and magnetic study of the $Nd_{2-x}Sr_xNiO_{4+\delta}$ system was undertaken to investigate the effects of Sr^{2+} substitution on the structural and physical properties of $Nd_{2-x}Sr_xNiO_{4+\delta}$. Because of the similarities between $Nd_2NiO_{4+\delta}$ and $La_2CuO_{4+\delta}$ (the parent compound of the $La_{2-x}M_xCuO_{4+\delta}$ superconductor family, M = alkaline earth ions), and of the recent reports of possible superconductivity in $La_{2-x}Sr_xNiO_{4+\delta}$ (*18*), a good understanding of the $Nd_{2-x}Sr_xNiO_{4+\delta}$ system should help in the understanding of these related systems.

Experimental

Solid–solutions of $Nd_{2-x}Sr_xNiO_{4+\delta}$ for various values of x ranging from 0 to 1 were prepared by codecomposition of the metal nitrates. Stoichiometric quantities of Nd_2O_3 (Aldrich, 99.9%), NiO (Aldrich, 99.99%), and $Sr(NO_3)_2$ (Aldrich, 99+%) were mixed together and dissolved in concentrated nitric acid. The excess nitric acid was removed by gradual heating and the resulting green solid was calcined in air at 800°C. The products were ground and heated in air at 1150°C for 32 hr in alumina crucibles with two intermittent grindings. The samples were cooled to 800°C in the furnace before being quenched to room temperature. The product was finally ground and cold pressed into pellets. The pellets were fired at 1150°C for 16 hr and slow cooled to room temperature.

Powder X-ray diffraction (XRD) data, collected on a SCINTAG PAD V diffractometer with monochromatized Cu$K\alpha$ radiation, were used to monitor the completion of the reaction. Least-squares refinement of

the observed powder diffraction data ($10° \leq 2\theta \leq 85°$) was used in the evaluation of cell parameters. Electrical resistivity of samples was measured by the standard four-probe technique in a DE202 cryostat (APD Cryogenics) from room temperature to 15 K. A SQUID magnetometer (Quantum Design) was used to measure the magnetic susceptibility of samples in the temperature region 2–370 K at an applied magnetic field of 1000 g. The total oxygen content was determined by hydrogen reduction using a DuPont 951 thermogravimetric analyzer; the material was heated on a platinum pan in flowing 5% H_2 in helium gas (0.1 liter/min) to 1000°C at 10°C/min.

Results and Discussion

Structural

Single phase specimens in the $Nd_{2-x}Sr_xNiO_{4+\delta}$ solid–solutions were prepared by the codecomposition of component nitrates as evident by X-ray diffraction patterns. Lehmann and Müller-Buschbaum (*15*) have reported that $Nd_2NiO_{4+\delta}$ crystallizes with orthorhombically distorted K_2NiF_4-type structure (space group *Abma*). The orthorhombic distortion manifests itself in the splitting of some of the *hk*0-type reflections in the powder X-ray diffraction patterns. $NdSrNiO_4$, as previously reported (*16, 17*), possesses a tetragonal K_2NiF_4-type structure (space group *I*4/*mmm*), with no apparent splitting in the *hk*0 reflections. The degree of divergence in the *hk*0 reflections of the orthorhombic specimens served as an indicator of the degree of distortion from tetragonal symmetry. The powder X-ray diffraction patterns for $x \approx 0.2$ show no splitting of the *hk*0 reflections in the range $5° < 2\theta < 60°$, which is indicative of a phase transition from orthorhombic to tetragonal symmetry. Even though the low angle reflections did not show divergence in the *hk*0 reflections, the high angle data showed peak broadening in the corresponding reflections indicating that the actual symmetry could be lower than tetragonal.

The cell parameters as determined from the least-squares refinement of the PXD data are presented in Table I. The unit cell parameters for the end members agree well with those reported in the literature (*14, 16, 19*). The changes in the unit cell parameters a, c, and volume, as a function of x, are illustrated in Figs. 2a, 2b, and 2c, respectively. The tetragonality ratio c/a_t as a function of x is plotted in Fig. 3. The a_t for the orthorhombic samples were calculated using the expression $a_t = (a + b)/2\sqrt{2}$. It is evident from Table I that the orthorhombic to tetragonal phase transition in $Nd_{2-x}Sr_xNiO_{4+\delta}$ is achieved via a rapid compression in the b-unit cell parameter while the a cell parameter remains nearly unchanged. The unit cell volume decreases in the series even though Sr^{2+} ($r_{Sr^{2+}} = 1.45$ Å for CN = (IX)) is larger than Nd^{3+} ($r_{Nd^{3+}} = 1.303$ Å for CN = (IX)) (*20, 21*). The partial oxidation of Ni^{2+} ($r_{Ni^{2+}} = 0.83$ Å for CN = (VI)) to Ni^{3+} ($r_{Ni^{3+}} = 0.70$ Å for CN = (VI)) low spin case or ($r_{Ni^{3+}} = 0.74$ Å for CN = (VI)) high spin case (*20, 21*)) induced by the substitution of Sr^{2+} for Nd^{3+} more or less compensates for the size increase expected from the differences of ionic radii of Sr^{2+} and Nd^{3+}. Thus the volume should remain constant or increase slightly with increasing x. However, the volume decreases as a function of x probably due to factors other than ionic size effects. The variations of the tetragonal lattice parameters a and c show a clear dependence on x, although not in accordance with Vegard's rule. The a_t cell parameter decreases slowly in the range $0 \leq x \leq 0.2$, and thereafter decreases rapidly up to $x \approx 0.6$. A significant increase in the a_t parameter is evident for compositions with $x > 0.6$. The c cell parameter on the other hand remains nearly constant up to $x \approx 0.2$, increases monotonically up to $x \approx 0.6$, and then decreases with increasing x. The tetragonality c/a_t ratio also exhibits an increase from $x =$

TABLE I

STRUCTURAL AND PHYSICAL PROPERTIES OF $Nd_{2-x}Sr_xNiO_{4+\delta}$

Compound	a (Å)	b (Å)	c (Å)	Volume (Å)^3	c/a_t	Transition temperature (°C)
$Nd_2NiO_{4.16\pm0.03}$	5.3775(6)	5.441(1)	12.355(1)	361.52(7)	—	575
	(3.825)[a]			(180.76)[b]	(3.230)[b]	
$Nd_{1.95}Sr_{0.05}NiO_{4.12\pm0.03}$	5.374(1)	5.433(1)	12.353(3)	360.71(9)	—	495
	(3.821)[a]			(180.35)[b]	(3.233)[b]	
$Nd_{1.9}Sr_{0.1}NiO_{4.12\pm0.03}$	5.3733(7)	5.4292(9)	12.360(2)	360.56(6)	—	190
	(3.8193)[a]			(180.30)[b]	(3.236)[b]	
$Nd_{1.8}Sr_{0.2}NiO_{4.03\pm0.03}$	3.818(1)		12.357(9)	180.1(1)	3.237	
$Nd_{1.7}Sr_{0.3}NiO_{4.00\pm0.03}$	3.8020(7)		12.394(2)	179.16(5)	3.260	
$Nd_{1.6}Sr_{0.4}NiO_{3.97\pm0.03}$	3.7879(4)		12.437(2)	178.45(3)	3.283	
$Nd_{1.5}Sr_{0.5}NiO_{3.98\pm0.03}$	3.7757(4)		12.473(3)	177.81(4)	3.305	
$Nd_{1.4}Sr_{0.6}NiO_{4.00\pm0.03}$	3.7721(4)		12.479(3)	177.56(4)	3.308	
$Nd_{1.2}Sr_{0.8}NiO_{4.00\pm0.03}$	3.7812(4)		12.393(2)	177.19(3)	3.280	
$NdSrNiO_{4.00\pm0.03}$	3.7960(3)		12.303(2)	177.28(3)	3.240	

[a] The a_t for the orthorhombic samples were calculated using the expression $a_t = (a + b)/2\sqrt{2}$.
[b] Values for the orthorhombic samples were calculated using a_t instead of a.

0.2 to $x \approx 0.6$ then it decreases. Gopalakrishnan *et al.* (*22*) reported similar trends in the unit cell parameters for $La_{2-x}Sr_xNiO_4$. They observed an initial increase in the c parameter and a decrease in the a parameter for $0 < x < 0.5$. For $x > 0.5$, the c parameter decreased while the a cell parameter slightly increased. They attributed the trends in the cell parameters to be due to the changes in the electronic configuration of nickel. They assumed that the trivalent nickel exists in the low spin state. The initial increase in the c cell parameter (for $x \leq 0.5$) has been attributed to the Jahn–Teller distortions of the Ni^{3+} ions, with the single electron being localized in the d_{z^2} orbital. For samples with $x > 0.5$ the decrease in the c cell parameter was interpreted in terms of a crossover in the electronic configuration of Ni^{3+} ions from $t^6_{2g}d^1{}_{z^2}$ to $t^6_{2g}d^1{}_{x^2-y^2}$. The reason for this transition in the orbital occupancy was ascribed to lowering of energy, due to the greater covalent interaction between the nickel $d_{x^2-y^2}$ and $p\sigma$ orbitals of the oxide ions in the perovskite network. It is likely that in the present system the observed variations in the unit cell parameters can be explained by this model. Alternatively, the decrease in c cell parameter and simultaneous increase in the a cell parameters for $x > 0.5$ could also be understood in terms of electrostatic interactions between charged cations.

Tamura has reported a polymorphic transition in $Nd_2NiO_{4+\delta}$ at 847 K (*23*), corresponding to a structural phase transition to tetragonal symmetry. Subsequent studies have confirmed this transition from high temperature X-ray diffraction and DSC studies (*11*). In order to understand the influence of Sr^{2+} substitution on the nature of this phase transition we have carried out high temperature X-ray diffraction and DTA studies from room temperature to 850°C in controlled oxygen atmospheres for samples with $x \leq 0.2$. We observed that the high temperature orthorhombic to tetragonal phase transition was unaffected by the oxygen partial pressure both in the pure as well as in the Sr^{2+}-substituted samples. Incorpo-

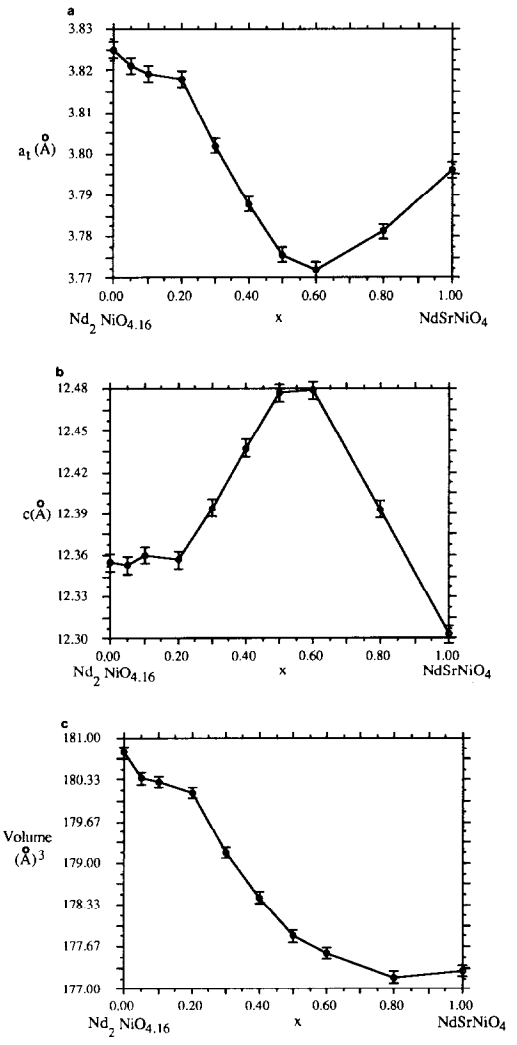

FIG. 2. (a) Change in the lattice parameter a as a function of Sr content in $Nd_{2-x}Sr_xNiO_{4+\delta}$. (b) Change in the lattice parameter c as a function of Sr content in $Nd_{2-x}Sr_xNiO_{4+\delta}$. (c) Change in the unit cell volume as a function of Sr content in $Nd_{2-x}Sr_xNiO_{4+\delta}$.

ration of Sr^{2+} in Nd_2NiO_4 resulted in a dramatic decrease in this transition temperature corresponding to the structural transformation (Table I). We see no evidence for a structural transition above room temperature for the tetragonal samples corresponding to $x \geq 0.2$. It is apparent that the

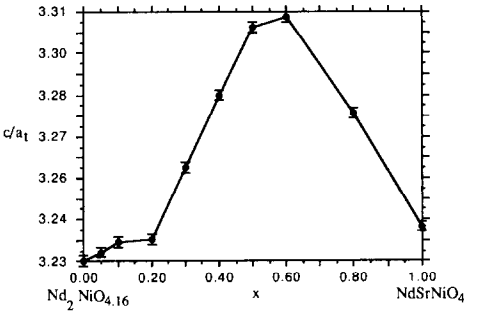

FIG. 3. Change in the c/a_t ratio as a function of Sr content in $Nd_{2-x}Sr_xNiO_{4+\delta}$.

high temperature tetragonal phase of Nd_2NiO_4 is stabilized by the incorporation of Sr^{2+}, although the exact mechanism responsible for this stabilization remains unclear at present.

Oxygen Content Analysis

In order to study the variations in the overall oxygen content as function of x in the $Nd_{2-x}Sr_xNiO_{4+\delta}$, we have carried out TGA studies in hydrogen atmospheres. A common feature in the reduction curves for all compositions was the observation of a step-like behavior. A representative weight-loss curve for $Nd_2NiO_{4.16}$ is illustrated in Fig. 4. The well-defined broad plateaus in the weight-loss curves are generally associated with the stabilization of several phases

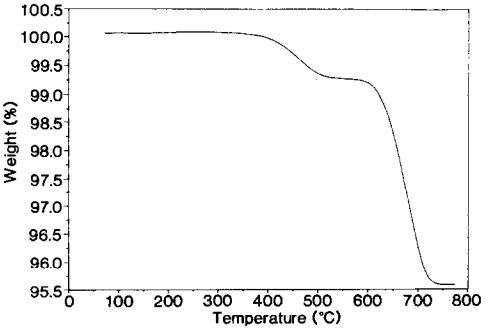

FIG. 4. Weight-loss curve for $Nd_2NiO_{4.16}$.

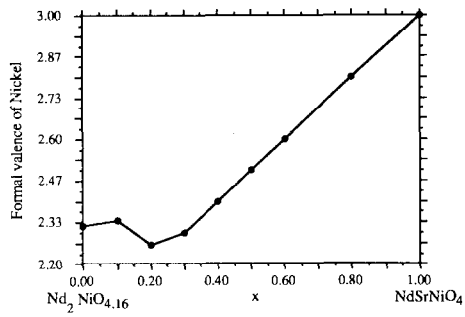

FIG. 5. Formal valence of nickel as a function of Sr content in $Nd_{2-x}Sr_xNiO_{4+\delta}$.

with varied oxygen stoichiometries (*6*). Oxygen contents were estimated across the series assuming Nd_2O_3, SrO, and metallic Ni as final products using the integrated peak intensities of the first derivatives of the weight changes and the corresponding values are given in Table I. It is clear from these values that the oxygen content remains close to four for the tetragonal compositions, while deviations from the ideal value are substantial in the orthorhombic compositions. This indicates that the stabilization of the K_2NiF_4 structure with orthorhombic distortion is achieved by incorporation of extra oxygens in the structure, whereas the tetragonal structure is stable with higher concentrations of Sr^{2+} and Ni^{3+} in the structure. Figure 5 shows the formal valence of nickel (estimated from the oxygen analysis) plotted against x. The formal valence of nickel increases linearly with the amount Sr^{2+} substitution for samples with $x > 0.2$, while the same remains nearly constant in the range $0 \leq x \leq 0.2$.

The stability of K_2NiF_4 structures are often described in terms of the tolerance factor defined as (*24*)

$$t = \frac{r_{A-O}}{\sqrt{2}\, r_{B-O}}$$

where $r_{(A-O)}$ and $r_{(B-O)}$ refer to the sum of covalent radii of A–O and B–O bonds in nine and six coordination, respectively. The K_2NiF_4 structure is stable over the range $0.85 < t < 1$, which is consistent with the absence of rare earth nickelates with the smaller rare earth ions (e.g., Sm, Eu, Gd . . .). The value of t is very close to the lower limit for Ln_2NiO_4 (Ln = La, Pr, and Nd), thus explaining the deviations from the ideal tetragonal geometry. It is possible to increase the value of t by either increasing the effective radii of A ions (substituting larger divalent alkaline earth ions at the rare earth sites), or by partially oxidizing the B cations to higher valence states by suitable substitutions at both A and/or B sites. Based on the oxygen analysis of the samples (Table I), the excess oxygen observed for the compositions with $x < 0.2$ promotes the partial oxidation of Ni^{2+}, thereby decreasing the $r_{(B-O)}$ values and consequently stabilizing the structure. Note, that for samples with $x > 0$, the oxygen content decreases so that in the $0 < x \leq 0.2$ region the Sr^{2+} and Ni^{3+} size effects play an increasing role in stabilizing the phase. For compositions with $x > 0.2$ both the formal valence of nickel and increased $r_{(A-O)}$ value are sufficient to stabilize the tetragonal structure, which account for the invariance of the oxygen stoichiometry in these samples. It is likely that the orthorhombic to tetragonal-like transition seen at $x \approx 0.2$ can be associated with changes in the values of the tolerance factor. The complex variations in the cell parameters with $x > 0.2$ for the $Nd_{2-x}Sr_xNiO_{4+\delta}$ system appear not to correspond with the overall oxygen content and hence can be ascribed to electronic instabilities alone as discussed earlier.

Electrical Transport Behavior

The room temperature resistivity (ρ_{RT}) values as a function of x are presented in Fig. 6. As can be seen, the room temperature resistivity of the samples decreases with increasing x. This observation correlates well with changes in the formal valence of nickel

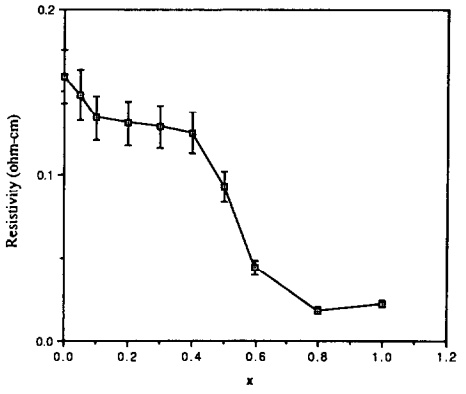

FIG. 6. Room temperature electrical resistivity as a function of Sr content in $Nd_{2-x}Sr_xNiO_{4+\delta}$.

(Fig. 5), as a function of x, demonstrating the influence of mixed valent nickel on the room temperature properties.

It is worth noting that the room temperature resistivity displays a decrease with increasing x, which is not parallel with the changes in the cell parameters. This behavior contrasts with the observations for the $La_{2-x}Sr_xNiO_4$ series where the room temperature resistivity is shown to follow the same trends as the cell parameter changes (*22*). In the polycrystalline samples the room temperature resistivity is expected to vary with the size and shape of the grain boundaries and hence precise estimation of the ρ_{RT} values is often complicated, thus data on single crystals would be of help in resolving the differences between the Sr^{2+}-substituted La and Nd nickelate systems.

The variation of log ρ vs $1/T$ for selected samples, measured in the range 10–300 K, is presented in Fig. 7. Except for $NdSrNiO_4$, which undergoes a metal-to-semiconductor transition at 190 K, all the members of the solid–solution series are semiconducting down to 10 K. The activation energies estimated from the plots of log ρ vs $1/T$ (125 to 300 K) show gradual decrease with increasing x across the series. The decreasing slope of log ρ vs $1/T$ seen at low temperatures is characteristic of an increasing dominance of extrinsic effects on the transport properties. The decrease in the activation energies in the high temperature region going from $Nd_2NiO_{4.16}$ to $NdSrNiO_4$ appears to indicate the increased delocalization of the Ni^{3+} electrons.

$NdSrNiO_4$ exhibits metallic-like behavior in the temperature interval 190–300 K. This is consistent with the configurational transition $t^6_{2g}d^1{}_{z^2} \rightarrow t^6_{2g}d^1{}_{x^2-y^2}$ suggested earlier, since the $\sigma^*{}_{x^2-y^2}$ band proposed for the electronic structure of $Nd_2NiO_{4+\delta}$ (Fig. 8), would be completely depleted for $x = 1$, and in the d_{z^2} narrow band of Ni^{3+} the electrons would be localized (*25*). Thus it seems that in $NdSrNiO_4$ there is a half-filled $\sigma^*{}_{x^2-y^2}$ band responsible for the metallic behavior. At ~190 K there is a metal-to-semiconductor transition and the resistivity increases rapidly with decreasing temperature. The metal–semiconductor transition may be associated with a charge density wave instability inherent in a half-filled band, or it may be due to other localization effects. These observations are qualitatively in agreement with those reported for $NdNiO_3$ (*26*) in which a metal–semiconductor-like transition was reported at ~130 K. The value of ρ_{RT} for $NdSrNiO_4$ (4×10^{-3} Ω cm) is about an order of magnitude smaller than that of $NdNiO_3$ (1.5×10^{-2} Ω cm), which contrasts with the generally held view that in its room temperature state the A_2BO_4 phase exhibits higher resistivity than its perovskite analog ABO_3 (*27*). In the absence of precise measurements of ρ_{RT} on single crystalline samples it is difficult to comment further on these observations.

Magnetic Properties

The dependence of normal state magnetic susceptibility ($\chi_{300\,K}$) on the value of x is illustrated in Fig. 9. The decrease in the $\chi_{300\,K}$ values with increasing x can be understood in view of the fact that the paramagnetic Nd^{3+} ions are being progressively re-

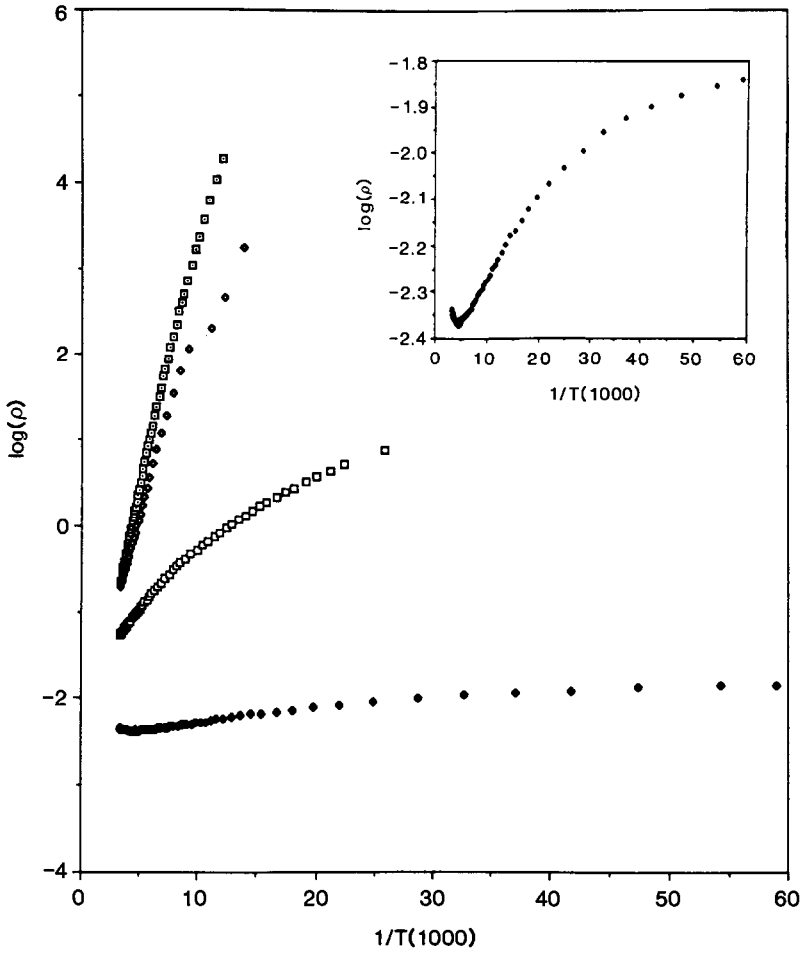

FIG. 7. The log(ρ) versus inverse temperature for ⊡: $x = 0$; ◆: $x = 0.4$; ■: $x = 0.6$; ◆: $x = 1$ in $Nd_{2-x}Sr_xNiO_{4+\delta}$. The insert shows the metallic behavior of the sample with $x = 1$.

placed by diamagnetic Sr^{2+} ions. It is interesting to note that the decrease in the $\chi_{300\,K}$ values for the orthorhombically distorted compositions is relatively small, whereas a dramatic decrease is observed for the tetragonal specimens with increasing x. The anomalies seen in the $\chi_{300\,K}$ values near $x \approx 0.2$ may be also related to the orthorhombic to tetragonal structural phase transition. Moreover, the changes in the $\chi_{300\,K}$ with x correspond well with the variations in the a cell parameter at least for the compositions in the range $0 \leq x \leq 0.5$, indicating that the magnetic properties are very sensitive to the Ni–O bond distances in the basal plane.

Variation of the magnetic susceptibility with temperature in the range 2–370 K are shown in Fig. 10 for selected members of the $Nd_{2-x}Sr_xNiO_{4+\delta}$ system. The susceptibility values were not corrected for the core diamagnetism of the component ions because of the large paramagnetic contribution from the Nd^{3+} ions. We see no evidence for a long range magnetic order down to 2 K in the end members $Nd_2NiO_{4.16}$ and NdSr-

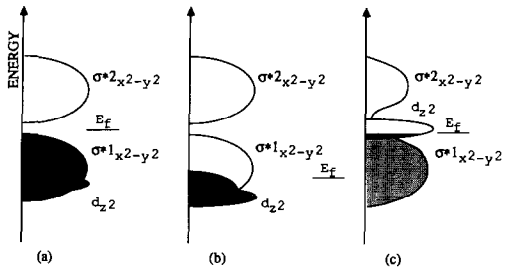

FIG. 8. Schematic density of states vs energy diagram for the σ-bond $3d$ electrons of Nd_2NiO_4 (after Ref. (*25*)). Not shown are filled O^{2-} $2p^6$, Nd $4f^3$, and Ni^{2+} t^6_{2g} bands and empty Ni $4s$ and Nd^{3+} $6s$ and $5d$ bands; (a) $\sigma^*_{x^2-y^2}$ band split by electron correlations or a charge density wave; (b) emptying of the $\sigma^*_{x^2-y^2}$ band and lowering of d_{z^2} band with increasing Sr^{2+} content in $Nd_{2-x}Sr_xNiO_4$; (c) configuration transition of band structure from $t^6_{2g}d^1{}_{z^2}$ to $t^6_{2g}d^1{}_{x^2-y^2}$ resulting in metallic properties.

NiO_4. The absence of a long range magnetic order in $Nd_2NiO_{4.16}$ is consistent with the observations of Buttrey and Honig (*4*), who showed that the magnetic order of the nickel sublattice can be suppressed with large excess of oxygen in the structure. However, sharp anomalies in the χ vs T plots, indicative of antiferromagnetic ordering (T_N = 17 K), are evident in the compositions corresponding to $0.4 \leq x \leq 0.7$.

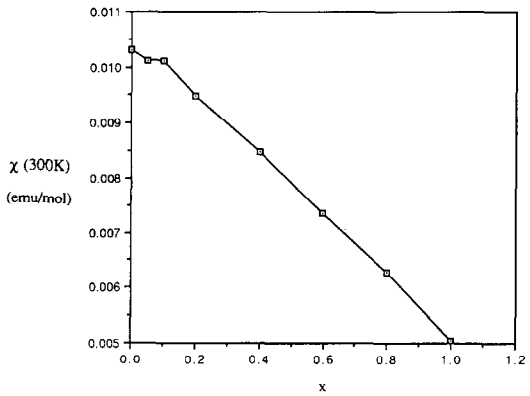

FIG. 9. Magnetic susceptibility at 300 K as a function of Sr content in $Nd_{2-x}Sr_xNiO_{4+\delta}$.

The susceptibility data in the temperature range 220–370 K can be fitted to the Curie–Weiss equation

$$\chi = C/(T + \Theta) + \chi_0,$$

where C and Θ are the Curie and Weiss constants, respectively, and the term χ_0 includes the temperature-independent contribution of the Pauli paramagnetic susceptibility, core diamagnetism, and the Van Vleck susceptibility. Any deviations in the Curie–Weiss behavior can be best seen in the plots of $1/\chi$ vs T, which are presented in Fig. 11. The Weiss constants for all the samples were estimated from a least-squares analysis performed on the linear portion of the graphs in the temperature range 220–370 K. The corresponding values are reported in Table II.

The deviations from the ideal Curie–Weiss behavior are clearly seen in the plots of $1/\chi$ vs T (Fig. 11) below 100 K. These deviations are attributable to the crystal field splitting of Nd^{3+}, J = 9/2 ground state; the susceptibility being determined from the relative population of these levels at different temperatures. Accordingly, we have limited the temperature range to 220–370 K for the estimation of C and Θ values. The μ_{eff} values derived from the Curie constants are listed in Table II together with the theoretically expected moments for Nd^{3+}. The differences in the observed and calculated μ_{eff} values, $\Delta\mu_{eff}$, are also presented in Table II.

It is seen that the Weiss constant remains negative for all the compositions, indicating that the dominant exchange interactions are antiferromagnetic. The Θ value (-90 K) obtained for $Nd_2NiO_{4.16}$ in the present study appears to be slightly higher than values reported before on the same compound (-50 K, -18 K) (*4*, *28*) in the same temperature interval. A comparison of the Θ values for Nd_2NiO_4, reported by several authors including the present study, suggests that the strength of antiferromagnetic exchange in-

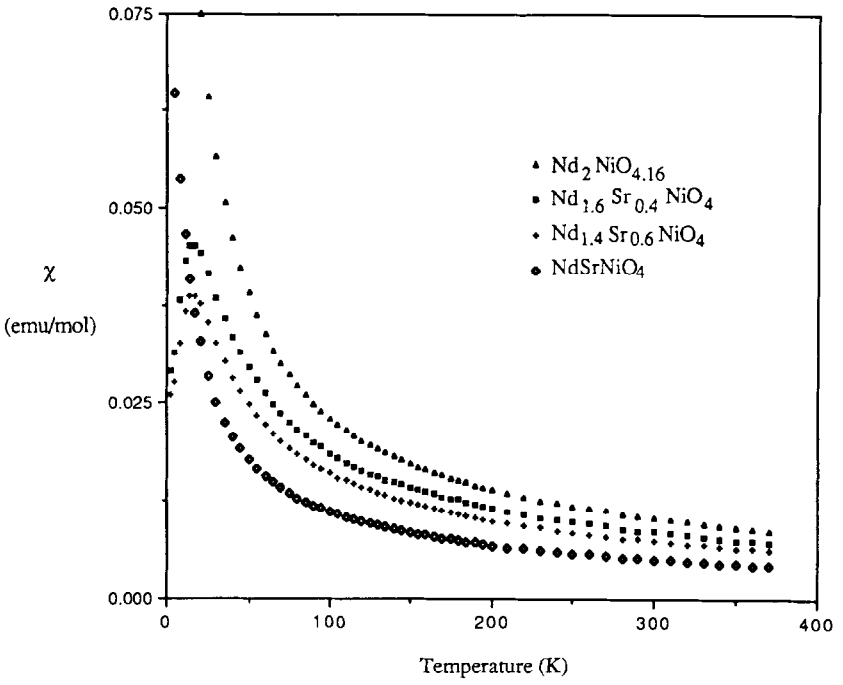

FIG. 10. Magnetic susceptibility versus temperature of $Nd_2NiO_{4.16}$, $Nd_{1.6}Sr_{0.4}NiO_4$, $Nd_{1.4}Sr_{0.6}NiO_4$, and $NdSrNiO_4$.

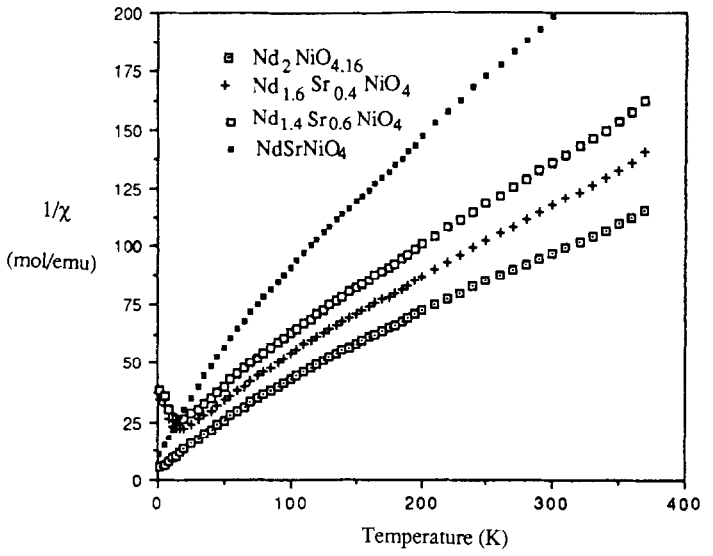

FIG. 11. The inverse suscpetibility versus temperature for $Nd_2NiO_{4.16}$, $Nd_{1.6}Sr_{0.4}NiO_4$, $Nd_{1.4}Sr_{0.6}NiO_4$, and $NdSrNiO_4$.

TABLE II

MAGNETIC PROPERTIES FOR $Nd_{2-x}Sr_xNiO_{4+\delta}$ IN THE TEMPERATURE RANGE 220–370 K[a]

Compound	μ_{eff} (μ_β) observed	μ_{eff}(μ_β) calculated	$\Delta\mu$(μ_β)	θ (K)
$Nd_2NiO_{4.16\pm0.03}$	4.002	3.62	0.38	−90.3
$Nd_{1.95}Sr_{0.05}NiO_{4.12\pm0.03}$	3.990	3.53	0.46	−95
$Nd_{1.9}Sr_{0.1}NiO_{4.12\pm0.03}$	3.898	3.44	0.46	−78
$Nd_{1.8}Sr_{0.2}NiO_{4.03\pm0.03}$	3.826	3.26	0.57	−86.2
$Nd_{1.6}Sr_{0.4}NiO_{3.97\pm0.03}$	3.599	2.89	0.706	−83
$Nd_{1.5}Sr_{0.5}NiO_{3.98\pm0.03}$	3.469	2.715	0.754	−70
$Nd_{1.4}Sr_{0.6}NiO_{4.00\pm0.03}$	3.358	2.534	0.824	−84.5
$Nd_{1.2}Sr_{0.8}NiO_{4.00\pm0.03}$	3.100	2.172	0.928	−84.8
$NdSrNiO_{4.00\pm0.03}$	2.812	1.81	1.002	−91.8

[a] These values reflect the contribution from Nd^{3+} ions alone. No correction for crystal field effects were applied.

teractions are extremely sensitive to the total oxygen content of the compound. For stoichiometric $Nd_2NiO_{4+\delta}$ ($\delta \approx 0$), $\Theta \approx -18$ K, and it increases with increasing δ. The increase of Θ with δ is consistent with the corresponding decrease in the unit cell volume. However caution should be exercised in the comparison of Θ values obtained for samples with varied oxygen contents due to the observation of ferromagnetic order in nearly stoichiometric specimens (*2*). Moreover, the large crystal field splitting effects of Nd^{3+} ($J = 9/2$) coupled with the changes in the type of magnetic order in the Ni sublattice with temperature may also account for the spread in the Θ values reported by different authors.

The magnetic moment of 4.0 μ_β observed for $Nd_2NiO_{4.16}$ is slightly higher than the value expected from the contribution of Nd^{3+} ions alone (3.62 μ_β). The difference between the observed and calculated magnetic moments in this compound ($\Delta\mu_{eff} = 0.38\ \mu_\beta$) can be attributed to the contribution from the Ni^{2+}/Ni^{3+} sublattice. Such a small value of $\Delta\mu$ suggests that the nickel sublattice is ordered antiferromagnetically (AF) well above the temperature range of the present investigation. As can be seen (Fig. 12), the $\Delta\mu_{eff}$ increases with x in $Nd_{2-x}Sr_xNiO_{4+\delta}$, implying increased contribution of the Ni^{2+}/Ni^{3+} sublattice to the total μ_{eff} as Sr^{2+} is progressively incorporated in Nd_2NiO_4. With increasing x, the AF ordering is frustrated and the magnetically bound electrons are released, which accounts for the observed increase in $\Delta\mu_{eff}$. Nevertheless, the $\Delta\mu_{eff}$ values calculated for different values of x in $Nd_{2-x}Sr_xNiO_4$ are too small to account for the complete localization of electrons in the *ab* plane. For example, the composition $NdSrNiO_4$, presumably having all the nickel in trivalent state, has a $\Delta\mu_{eff}$ value close to 1 μ_β, smaller than 1.73 μ_β expected for low spin Ni^{3+} ($S = \frac{1}{2}$). In light of these observations, it is reasonable to assume that in $Nd_{2-x}Sr_xNiO_4$ the electrons in the nickel sublattice are partially delocalized which is consistent with their electrical transport properties, the band structure proposed for Ln_2NiO_4 (Fig. 8, Ref. (*25*)) and the transition of electronic configuration of the *d* manifold electron structure proposed for $x > 0.6$.

Prior to this study, there were no reports on the long range magnetic order of the rare earth sublattice from magnetization measurements in Ln_2NiO_4 compounds, although Rodríguez-Carvajal *et al.* (*29*) have proposed $T_N \approx 10$ K for Nd_2NiO_4 based on temperature-dependent neutron diffraction

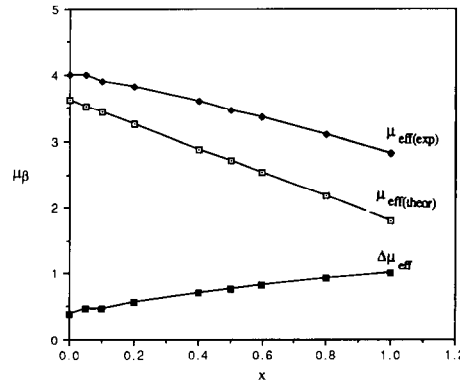

FIG. 12. $\mu_{eff(exp)}$, $\mu_{eff(theor)}$, and $\Delta\mu_{eff}$ as a function of Sr content in $Nd_{2-x}Sr_xNiO_{4+\delta}$.

studies. However, they reported that the long range magnetic order is destroyed in fully oxidized samples of $Nd_2NiO_{4+\delta}$ ($\delta > 0.04$) in agreement with the results reported in this study. Although the end members of the solid–solution series $Nd_{2-x}Sr_xNiO_{4+\delta}$ ($x = 0$; $x = 1$) did not display static 3D magnetic structure down to 2 K, it is evident that the compositions with $0.4 < x < 0.6$ have a well-defined long range order (T_N = 17 K) indicative of antiferromagnetic interactions. Furthermore, the samples corresponding to $x = 0.8$ and 0.3 showed small anomalies in the χ vs T plots at ~8 K. It is worth noting in this context that we do not see anomalies in the χ vs T plots at 190 K in $NdSrNiO_4$ where the electrical resistivity shows a transition from metallic to semiconducting behavior. It is possible that the strong paramagnetic moments of Nd^{3+} ions mask small discrepancies in the χ values, as has been proposed for the analogous $NdNiO_3$ system.

According to Rodríguez-Carvajal *et al* (*29*), the presence of long range magnetic order in the Nd_2NiO_4 system can be explained in terms of the relative strengths of local exchange fields of the type J_{Ni-Nd} and J_{Nd-Nd}. At higher temperatures the strong local fields originating from the polarization of the Nd sublattice by Ni^{2+} ions prevent any 3D static magnetic order between the rare earth ions (i.e., $J_{Ni-Nd} > J_{Nd-Nd}$). However, at relatively lower temperatures the onset of magnetic order can be attributed to the dominant J_{Nd-Nd} type of interactions. In addition it is proposed that the oxygen stoichiometry is extremely critical for the existence of long range magnetic order of the Nd sublattice, which is also consistent with the absence of magnetic order in orthorhombic $Nd_{2-x}Sr_xNiO_{4+\delta}$ where δ is > 0. This implies that in the compositions with orthorhombically distorted structures, the extra oxygen produces severe distortions in the local coordination of the cations which would frustrate the long range magnetic order of the rare earth ions. The observation of a well-defined T_N in the samples with tetragonal geometry ($\delta = 0$) is consistent with this model. The absence of magnetic order in $NdSrNiO_4$ may be related to dilution effects, i.e., long range magnetic interactions between the rare earth ions are interrupted by the Sr^{2+} ions. It is puzzling to note that T_N and Θ remains constant in the samples for $0.4 \leq x \leq 0.7$, although significant variations in the cell parameters are apparent in this range. Detailed studies aimed at characterizing the antiferromagnetic transition observed in some of the intermediate members of the solid–solution series are currently in progress.

Conclusion

In summary, we have successfully synthesized a new solid–solution series of $Nd_{2-x}Sr_xNiO_{4+\delta}$ ($0 \leq x \leq 1$ and $0.16 \leq \delta \leq 0$) by the codecomposition of component nitrates and studied their structural and physical properties. From the powder X-ray diffraction studies it was evident that at $x \approx 0.2$, there appears to be a structural phase transition from orthorhombic to pseudo-tetragonal symmetry. The unit cell parameters a and c displayed anomalous variations with x, suggestive of electronic instabilities originating from the configurational changes in the d-manifold of the Ni ions. The high temperature structural phase transition observed for $Nd_2NiO_{4+\delta}$ at ~847 K was suppressed rapidly with the incorporation of Sr^{2+} in the structure. Oxygen analysis indicated substantial deviations from the ideal values for the orthorhombically distorted samples (i.e., $0 \leq x \leq 0.2$), although near-ideal stoichiometries were seen in the tetragonal specimens. Large values of δ ($0 \leq \delta \leq 0.2$) in the orthorhombic members of the series appear to be necessary for the stabilization of the K_2NiF_4-type structure which may be deduced from the tolerance factor considerations. Electrical resistivity mea-

surements indicated a gradual change in the transport behavior from semiconducting to semimetallic with progressive increase of Sr^{2+} content in $Nd_2NiO_{4+\delta}$. $NdSrNiO_4$ showed a metal–semiconductor transition at ~190 K, possibly related to the onset of a charge density wave characteristic of half-filled conduction band. The room temperature resistivity also exhibits an anomalous decrease at the structural phase transition near $x \approx 0.2$. The temperature-dependent magnetic susceptibility measurements are indicative of a 3D long range antiferromagnetic order ($T_N \approx 8$–17 K) of the Nd sublattice for several intermediate members with tetragonal symmetry. Deviations from the ideal Curie–Weiss behavior seen in the $1/\chi$ vs T plots below 100 K have been ascribed to the crystal field effects of Nd^{3+} ion ($J = 9/2$). The difference between the observed and calculated magnetic moments ($\Delta\mu_{eff}$) increases with increasing x in $Nd_{2-x}Sr_xNiO_4$ which is attributed to the frustrations of AF pairing that originate from the mixed valence of Ni^{2+}/Ni^{3+}. The observation of T_N in several compositions with tetragonal structure was qualitatively interpreted in terms of changes in the strengths of exchange interactions of the type $J_{Nd(Sr)-Nd(Sr)}$, $J_{Nd(Sr)-Ni}$; however, more detailed studies are necessary to understand the complex electronic behavior seen in the present system.

Acknowledgments

The authors thank Shu Li and Professor W. H. McCarroll for helpful discussions and critical evaluation of the manuscript. The work was supported by National Science Foundation Solid State Chemistry Grant DMR-8714072.

References

1. JM. Bassat, P. Odier, and F. Gervais, *Phys. Rev. B* **35,** 7126 (1987).
2. D. J. Buttrey, J. M. Honig, and C.N. R. Rao, *J. Solid State Chem.* **64,** 287 (1986).
3. C. N. R. Rao, D. J. Buttrey, N. Otsuka, P. Ganguly, H. R. Harrison, C. J. Sandberg, and J. M. Honig, *J. Solid State Chem.* **51,** 266 (1984).
4. D. J. Buttrey and J. M. Honig, *J. Solid State Chem.* **72,** 38 (1988).
5. P. Odier, Y. Nigara, and J. Coutures, *J. Solid State Chem.* **56,** 32 (1985).
6. J. T. Lewandowski, R. A. Beyerlein, J. M. Longo, and R. A. McCauley, *J. Amer. Ceram. Soc.* **69,** 699 (1986).
7. J. Drennan, C. P. Tavares, and B. C. H. Steele, *Mater. Res. Bull.* **17,** 621 (1982).
8. J. D. Jorgensen, B. Dabrowski, Shiyou Pei, D. R. Richards, and D. G. Hinks, *Phys. Rev. B* **40,** 2187 (1989).
9. J. Rodríguez-Carvajal, J. L. Martínez, J. Pannetier, and R. Saez-Puche, *Phys. Rev. B* **38,** 7148 (1988).
10. R. Saez-Puche, J. L. Rodriguez, and F. Fernandez, *Inorg. Chim. Acta.* **140,** 151 (1987).
11. R. Saez-Puche, R. Fernandez, and W. S. Glaunsinger, *Mater. Sci. Monogr. (React. Solid Pt. A)* **28,** 607 (1985).
12. P. Ganguly and C. N. R. Rao, *Mater. Res. Bull.* **8,** 405 (1973).
13. J. B. Goodenough and S. Ramasesha, *Mater. Res. Bull.* **17,** 383 (1982).
14. W. Bernard and D. Marc, *C. R. Acad. Sci., C* **267,** 1482 (1968).
15. U. Lehmann and Hk. Müller-Buschbaum, *Z. Naturforsch., B* **35,** 389 (1980).
16. G. Payom and M. Daire, *Rev. Chim. Miner.* **14,** 11 (1977).
17. G. Demazeau, M. Pouchard, and P. Hagenmuller, *J. Solid State Chem.* **18,** 159 (1976).
18. Z. Kakol, J. Spalek, and J. M. Honig, *J. Solid State Chem.* **79,** 288 (1989).
19. M. Foëx, *Bull. Soc. Chim. Fr.* **109** (1961).
20. R. D. Shannon and C. T. Prewitt, *Acta Crystallogr., Sect. B* **25,** 925 (1969).
21. R. D. Shannon, *Acta Crystallogr., Sect. A* **32,** 751 (1976).
22. J. Gopalakrishnan, G. Colsmann, and B. Reuter, *J. Solid State Chem.* **22,** 145 (1977).
23. S. Tamura, *J. Phys. Soc. Japan.* **33,** 574 (1972).
24. J. F. Ackerman, *Mater. Res. Bull.* **14,** 487 (1979).
25. J. B. Goodenough, *Mater. Res. Bull.* **8,** 423 (1973).
26. J. K. Vassiliou, M. Hornbostel, R. Ziebarth, and F. J. DiSalvo, *J. Solid State Chem.* **81,** 208 (1989).
27. C. N. R. Rao, P. Ganguly, K. K. Singh, and R. A. Mohan Ram, *J. Solid State Chem.* **72,** 14 (1988).
28. R. Saez-Puche, and F. Fernández, *Solid State Commun.* **72,** 273 (1989).
29. J. Rodríguez-Carvajal, M. T. Fernández-Díaz, J. L. Martínez, F. Fernández, and R. Saez-Puche, *Europhys. Lett.* **11,** 261 (1990).